NOTICE CONCERNING COPYRIGHT RESTRICTIONS

dramatically between parts b and c of Figure 3, although there is only a very small capillary pressure increment. The relative permeability for water changes almost like a step-function, and for a wide range of saturation the relative permeability for both phases is zero (not shown). This is the result of a few bottleneck fractures with large apertures that obstruct the advancement of the imbibition front due to the blocking assumption.

REFERENCES

Billaux, D., Bodea, S., and Long, J., 1989a. FMG, RENUM, LINEL, ELLFMG, ELLP, and DIMES: Chain of programs for calculating and analyzing fluid flow through two-dimensional fracture networks. Theory and design. Lawrence Berkeley Laboratory Report LBL-24914.

Billaux, D., Peterson, J., Bodea, S., and Long, J., 1989b. FMG, RENUM, LINEL, ELLFMG, ELLP, and DIMES: Chain of programs for calculating and analyzing fluid flow through two-dimensional fracture networks. Users manual and listings. Lawrence Berkeley Laboratory Report LBL-24915.

Karasaki, K., 1987. A new advection dispersion code for calculating transport in fracture networks. Earth Sciences Division Annual Report 1986. Lawrence Berkeley Laboratory Report LBL-22090, p. 55–58.

Kwicklis, E.M., and Healy, R.W., 1992. Numerical investigation of steady liquid water flow in a variably saturated fracture network. Paper submitted to Water Resour. Res.

Persoff, P., Pruess, K., and Myer, L., 1991. Two phase flow visualization and relative permeability measurement in transparent replicas of rough-walled rock fractures. *In* Proceedings, 16th Workshop on Geothermal Reservoir Engineering, Stanford, California, January 23–25, 1991 (LBL-30161).

Pruess, K., and Tsang, Y., 1990. On two-phase relative permeability and capillary pressure of rough-walled rock fractures. Water Resour. Res., v. 26, no. 9, p. 1915–1926 (LBL-27449).

Wilkinson, D., and Willemsen, J.F., 1983. Invasion percolation: A new form of percolation theory. J. Phys. A: Math. Gen. 16, p. 3365–3376.

6822

A Numerical Study of the Structure of Two-Phase Geothermal Reservoirs

C. H. Lai and G. S. Bodvarsson

Major two-phase vapor-dominated geothermal reservoirs have been exploited at The Geysers, California; Larderello, Italy; Matsukawa, Japan; and Kamojang, Indonesia. These reservoirs produce only steam and have nearly vapor-static pressure gradients at corresponding saturation temperatures. High observed upward heat transport in these reservoirs results from counterflows of vapor and liquid.

White et al. (1971) proposed a model involving counterflow of ascending steam and descending condensate that was elaborated upon by many investigators. In these models, boiling at a deep brine "water table" was assumed, with steam moving upward in large fractures along the pressure gradient produced by boiling and then condensing at the top of the reservoir because of conductive heat loss to the surface. The condensate flowed downward by gravity in the rock matrix and small fractures. However, recent discoveries in the northern part of The Geysers and some evidence from Larderello suggest that dry high-temperature rock underlies the vapor-dominated reservoir. Some wells in the Coldwater Creek field of The Geysers encounter a high-temperature zone (up to 347°C) only 200 m below the 245°C vapor-dominated reservoir. At Larderello, a number of deep wells show temperatures above 350°C.

The objectives of the present study are (1) to characterize possible thermodynamic states as well as flow structures and heat-transfer processes in typical vapor-dominated geothermal reservoirs and (2) to explain the thermodynamic conditions encountered in the high-temperature reservoirs observed in The Geysers and Larderello.

DESCRIPTION OF THE PROBLEM

A numerical study of steady-state two-phase geothermal reservoirs was performed using a two-dimensional vertical cross section of porous medium. The cross section is heated locally from below, reflecting situations where localized magmatic intrusion occurs beneath the reservoir. Figure 1 shows a schematic representation of the right half of the physical problem considered in the study. The cross

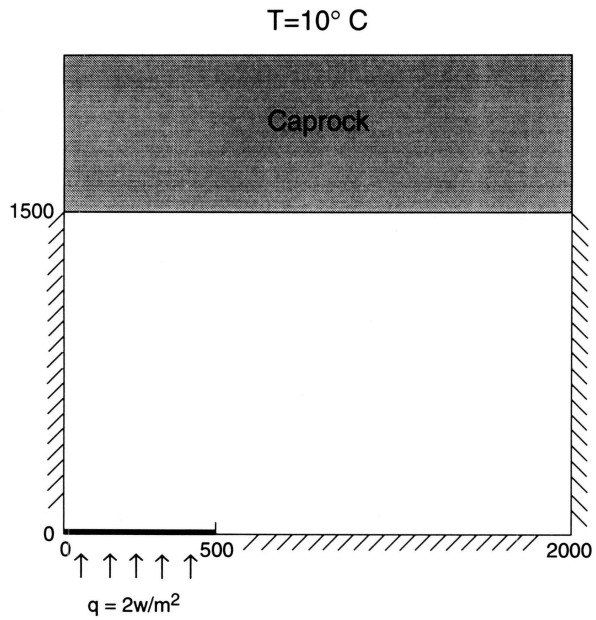

Figure 1. A schematic representation of the physical problem. [XBL 9112-7097]

section is overlain by an impermeable caprock, which is maintained at a constant temperature of 10°C at its top, representing the ground surface. Heat transfer in the caprock occurs only by conduction.

The numerical simulator TOUGH2 (Pruess, 1991a) was used with a uniform grid spacing of 100 m in both the x and z directions forming a 20×15 mesh. The parameters used in the simulations are considered to be appropriate for The Geysers and Larderello. The main parameters varied in the simulations were initial mass of *in situ* fluid and permeability.

Base Case: 25% Initial Steam Saturation

The phase structure may depend on the initial mass of *in situ* fluid (i.e., initial steam saturation). To test this hypothesis, numerical studies are performed to examine the effects of initial steam saturations on the phase and flow structures as well as on the heat-transfer process at steady-state conditions. In the numerical simulations, four cases with initial steam saturations of 25, 50, 70, and 75% and with a high permeability of 10^{-13} m^2 are designed to investigate the basic thermodynamic structures of the two-phase geothermal reservoirs. Cases 1, 2, 3, and 4 have steam saturations of 25, 50, 70, and 75%, respectively.

In case 1, the base case, we consider an initial steam saturation of 25% and a relatively high permeability of 10^{-13} m^2; under these conditions, the liquid tends to drain to the lower portion of the reservoir and the vapor to rise to the upper portion of the reservoir because of the large density difference between liquid and vapor, with the result that phase segregation occurs in the system. Figure 2a shows the steam saturation and mass flux distributions. Note that the mass flux shown in Figure 2 is generated by summing the mass flux in the liquid and steam phases. Examination of the figure reveals that two distinct zones with different steam saturations are developed in the reservoirs. In the upper two-phase vapor-dominated zone ($z > -500$ m), counterflow with an equal mass flux of steam (up) and liquid water (down) (i.e., a heat pipe) develops; the net mass flux in the two-phase zone is negligible compared with that in the underlying liquid zone ($z < -500$ m).

Figure 2b shows the temperature and mass flux distributions in the reservoir. The heat transfer in the liquid zone occurs by both conduction and convection. The adiabatic lateral boundary conditions and the constant heat flux imposed at the bottom surface serve to induce and sustain a buoyancy-driven flow in the vicinity of the heat source. As a result, a strong unicellular convective flow develops in the entire liquid zone, and the conduction-temperature field in the zone is greatly perturbed. Above the constant heat flux ($0 < x < 500$ m), the high-temperature isotherms shift toward the upper liquid zone ($-620 < z < -500$ m), resulting in a highly stratified region around $z = -560$ m.

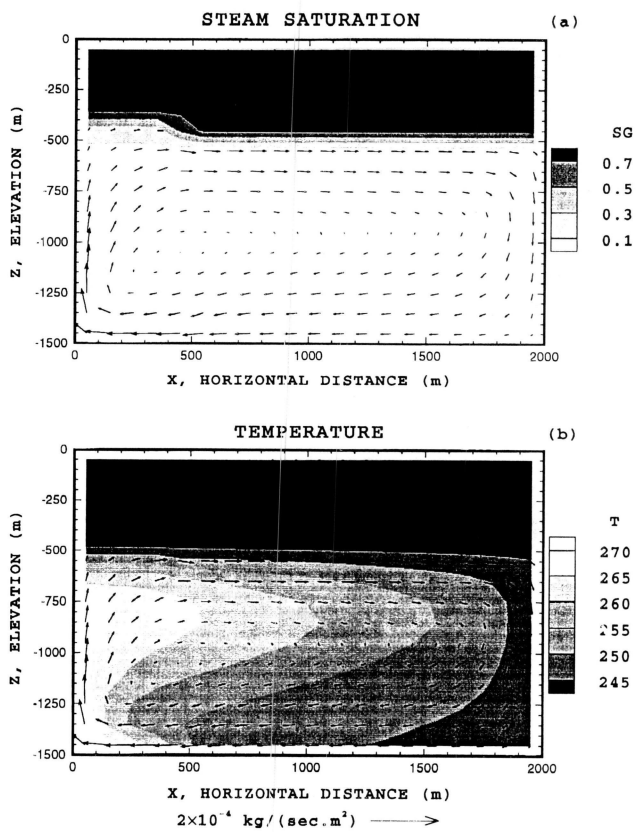

Figure 2. Distribution of (**a**) steam saturation (S) and mass flux and (**b**) temperature (T) and mass flux for case 1 with initial steam saturation of 25% and permeability of 10^{-13} m^2. [XBL 935-792]

Effect of Initial Steam Saturation

As the initial steam saturation increases to 50% (case 2), the initial mass of *in situ* fluid is decreased and the amount of mobile liquid water is reduced. Figure 3 shows the phase structure and distributions of temperature and mass flux. The interface between the liquid and two-phase zones is located at a depth of approximately 1050 m, and the thickness of the liquid zone is 450 m. Because the aspect ratio of the liquid zone (width over thickness) is larger than that derived from case 1, the convective cell is smaller and extends only over the left half of the zone. Consequently, the lateral extent of thermal activities is reduced and thus heat-transfer rates are decreased.

When the initial steam saturation is increased to 70% (case 3), a balanced liquid-vapor counterflow prevails in the entire reservoir. A small temperature variation of 240 to 245°C is observed in the system, indicating that the heat pipe efficiently dissipates the heat released from the heat source. However, when the steam saturation is increased to 75% (case 4), the amount of mobile liquid is further decreased and is not sufficient to produce a balanced liquid-vapor counterflow everywhere in the system. Figure 4 shows phase structure and distributions of the temperature and mass flux. Examination of these figures shows that a conduction-dominated zone develops in a region near the heat source; although a vapor convective flow field is observed, it is not as efficient as liquid convective flow to dissipate heat. Thus, a superheated vapor zone develops in the region near the heat source. This may reflect the situation where a superheated vapor zone underlies a two-phase zone in the Northern Geysers. The heat transfer in the two-phase zone overlying the superheated vapor zone is again by heat pipe.

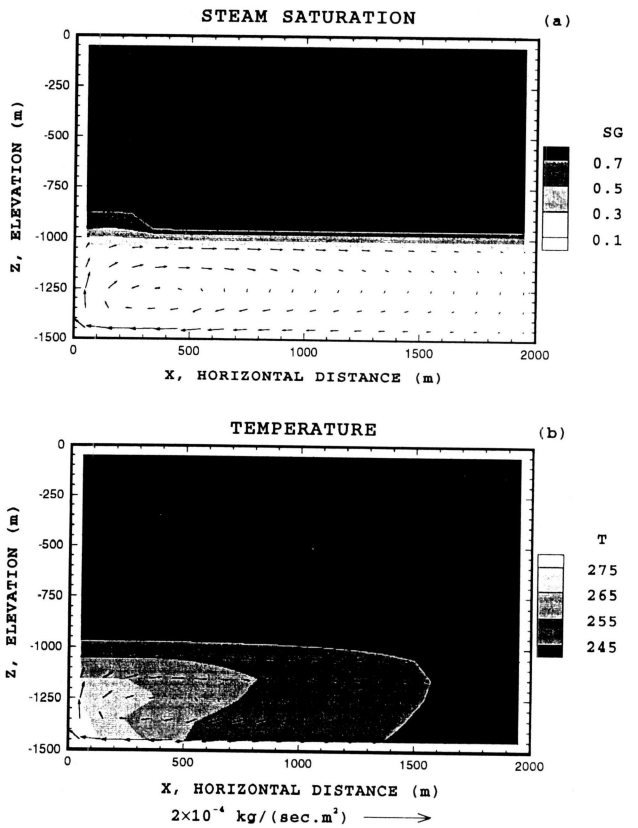

Figure 3. Distribution of (**a**) steam saturation (S) and mass flux and (**b**) temperature (T) and mass flux for case 2 with initial steam saturation of 50% and permeability of 10^{-13} m^2. [XBL 935-793]

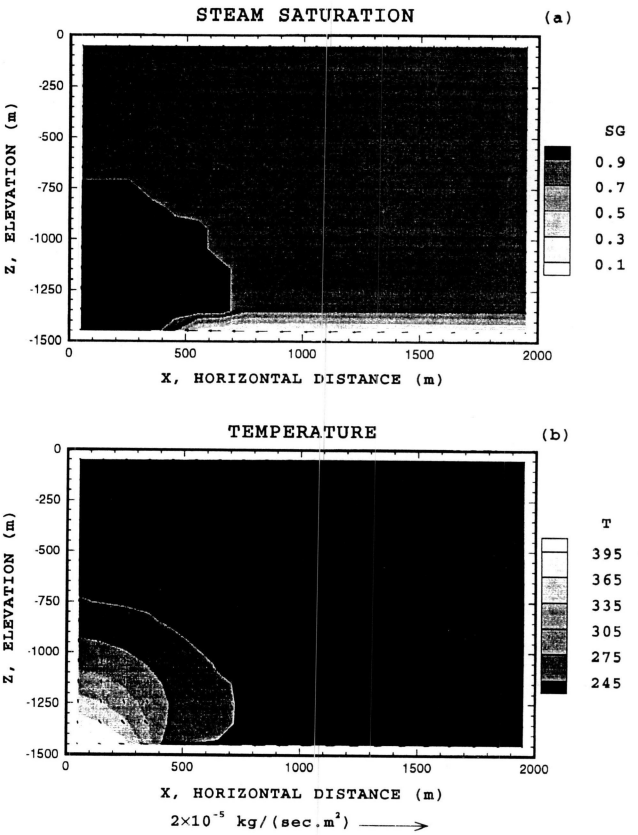

Figure 4. Distribution of (**a**) steam saturation (S) and mass flux and (**b**) temperature (T) and mass flux for case 4 with initial steam saturation of 75% and permeability of 10^{-13} m^2. [XBL 935-794]

Effect of Permeability

To investigate the effects of permeability on flow and heat-transfer processes, simulations are carried out with a permeability of 10^{-15} m^2 (case 5). An initial steam saturation of 25% is considered, with the rest of the physical parameters remaining the same as those used in case 1. In case 5, a conduction-dominated zone is developed in the region surrounding the heat source. Because heat conduction cannot efficiently dissipate the heat released from the heat source, a high-temperature zone of approximately 375°C occurs immediately above the heat source. This

results in the development of a boiling zone in a region above the heat source, as shown in Figure 5. The temperature and pressure profiles along the vertical cross section with $0 < x < 300$ m may reflect the situation observed in Olkaria, Kenya, where permeabilities are low and on the order of millidarcies (Bodvarsson et al., 1987). Contrary to the situation in cases 1 to 4, the temperature in the two-phase zone decreases with distance away from $x = 0$, resulting in a higher heat flow near the surface immediately above the heat source.

Effect of Grid Orientation

Experience with simulations of multiphase flow through porous media using the conventional five-point differencing scheme shows that in the vertical plane, the effect of grid orientation may be significant on predicted simultaneous movement of two fluids with a large density contrast (Pruess, 1991b; Lai and Bodvarsson, 1993). The lighter fluid tends to move along the vertical grid lines aligned with gravity, and the heavier one tends to sink down along the gravitational direction.

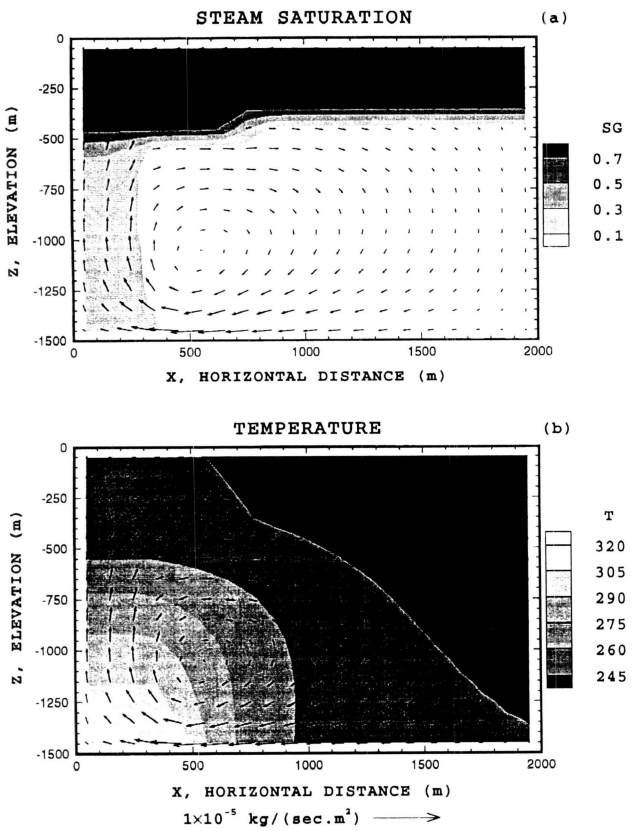

Figure 5. Distribution of (**a**) steam saturation (S) and mass flux and (**b**) temperature (T) and mass flux for case 5 with initial steam saturation of 25% and permeability of 10^{-15} m^2. [XBL 935-795]

To investigate the effects of grid orientation on our numerical simulation results, two different grid discretizations are used with so-called parallel and diagonal grids. For a parallel grid, the interface between the grid cells is either parallel or perpendicular to the gravitational direction. For a diagonal grid, the interface between the grid cells is oblique to the gravitational direction at 45 or 135 degree angles. We expect that the results calculated from case 5 possess a potential for grid orientation errors, because the vapor flow of the boiling zone immediately above the heat source tends to move vertically upward. As Figure 5 shows, this results in a zone with a relatively uniform width calculated with a parallel grid. However, the results derived from case 6 using a diagonal grid show that distribution of the temperature and saturation, and the shape of the boiling zone are only slightly different from those predicted from a parallel grid. Therefore, grid orientation effects for the present problem are probably insignificant.

CONCLUSIONS

The purpose of this work has been (1) to conduct a numerical study of flow, phase structure, and heat-transfer processes in natural-state two-phase geothermal reservoirs using a two-dimensional porous cross section with a localized heat flux from below as an idealized model for a geothermal system and (2) to analyze the effects of the mass of *in situ* fluid (i.e., initial steam saturation) and permeability on features of phase structure and heat-transfer processes.

The results show that when an initial steam saturation of 25% and a rather high permeability of 10^{-13} m^2 are employed, a two-phase vapor-dominated zone overlying a liquid zone develops. In the two-phase zone, a balanced liquid-vapor counterflow develops. The vapor rises to the top of the reservoir, where it condenses and releases latent heat, which is transferred through the caprock by conduction. The condensate either remains *in situ* or returns to the liquid zone. In the liquid zone, a convective flow field extends over the entire reservoir. The strength of the convective flow strongly depends on the mass of *in situ* fluid and the permeability of the reservoir. With an increase in initial steam saturation from 25 to 50%, the convective flow field extends only over the left half of the reservoir, resulting in lower heat-transfer rates. As the steam saturation is increased to 70%, a vapor-dominated heat pipe prevails in the entire system. When the steam saturation is increased to 75%, the amount of mobile liquid is reduced. Under such a circumstance, although a vapor convective flow develops, it is not as efficient as liquid convective flow in dissipating heat, resulting in a high-temperature superheated vapor zone underlying a two-phase vapor-dominated zone.

In general, the smaller the permeability considered in the model, the smaller the portion of the liquid zone affected by convective flow, leading to reduction of the rates of heat transfer. When a low permeability of 10^{-15} m^2 and an initial steam saturation of 25% are employed, conduction is the dominant heat-transfer mode in the liquid zone. Because heat released from the source cannot be efficiently dissipated by conduction, a two-phase liquid-dominated boiling zone develops immediately above it.

REFERENCES

Bodvarsson, G.S., Pruess, K., Stefansson, V., Bjornsson, S., and Ojiambo, S.B., 1987. East Olkaria geothermal field, Kenya: 1. History match with production and pressure decline data. J. Geophys. Res., v. 92, no. B1, p. 521–539 (LBL-20098).

Lai, C.H., and Bodvarsson, G.S., 1993. Numerical studies of cold water injection into vapor-dominated geothermal systems (to be published).

Pruess, K., 1991a. TOUGH2—A general-purpose numerical simulator for multiphase fluid and heat flow. Lawrence Berkeley Laboratory Report LBL-29400.

Pruess, K., 1991b. Grid orientation and capillary pressure effects in the simulation of cold water injection into depleted vapor zones. Geothermics, v. 20, p. 257–277, 1991 (LBL-30562).

White, D.E., Muffler, L.J.P., and Truesdell, A.H., 1971. Vapor-dominated hydrothermal systems compared with hot-water systems. Economic Geology, v. 66, p. 424–457.

6823

Modeling Flow and Transport for Stripa Phase III: What Did We Learn?

J. C. S. Long

The Stripa Project represents a major milestone in the development of technology for the characterization of fractured rock for the purpose of predicting fluid flow and transport. There is probably no other *in situ* block of rock of similar scale that has been probed in so many ways with such intensity in such a brief period of time. An examination of what was learned at Stripa is nearly equivalent to an examination of what is currently knowable about flow and transport in crystalline rock.

This article reviews a few of the key findings that involved fluid flow and transport modeling. The analyses are based on the conceptual model described in Olsson et al. (1989), Black (1991), and Olsson (1992). This model included the definition of the major fracture zones in the Site Characterization and Validation (SCV) rock block. In particular, the conceptual model identified the H-zone as a subvertical zone that was the only major fracture zone to intersect the Validation Drift (VD).

This discussion of model predictions will refer to three hydraulic experiments. The first is the set of cross-hole interference tests (Black, 1991) that took place between packed-off intervals of the SCV boreholes. In particular, we concentrate on the C1-2 test, whose source was confined to interval 2 in borehole C1, which intersected fracture zone H. The second experiment was the Simulated Drift Experiment (SDE) (Black et al., 1991), which was meant to mimic the behavior of a drift from the hydrologic point of view by placing six parallel boreholes within a ring. The third is the VD inflow experiment (Olsson, 1992), which was conducted from a drift excavated through one-half the length of the SDE boreholes. The SDE provided a unique study of the effects of excavation on hydrology.

The discussion will also refer to three sets of tracer experiments. The radar-saline experiments (Olsson, 1991a,b) consisted of combining a saline tracer test with radar tomography. In the first test, 30 l/min of saline was injected into the C1-2 interval and collected at a sink formed by opening the D-holes in the vicinity of the H-zone. The second test was a repeat of the first but took place after the excavation of the VD. The third set of tests consisted of tracer tests conducted after the excavation of the VD, where a variety of tracers were injected at very low rates from a variety of borehole intervals intersecting the H-zone and collected at the VD (Birgersson et al., 1992)

These experiments were used in the following ways. The C1-2 test was used to develop a model of fracture flow in the SDE based on the conceptual model of Black et al. (1991). The modeling approach used by LBL was to create hierarchical fracture systems through an iterative optimization procedure, or inverse method (Long et al., 1991, 1992a). In this approach, the fracture network is optimized so that it matches certain observations—for example, interference test results such as those from the C1-2 test. In